Sensitivities of future solar neutrino observatories to nonstandard neutrino interactions

Pouya Bakhti⦾ and Meshkat Rajaee

Institute for research in fundamental sciences (IPM), PO Box 19395-5531, Tehran, Iran

We study the matter effect caused by nonstandard neutrino interactions (NSI) in the future solar neutrino experiments, DUNE, HK, and MICA. The upcoming reactor experiment, JUNO is expected to provide the most precise measurements of solar neutrino oscillation parameters and is going to open up the era of subpercent precision in the leptonic mixing sector of the Standard Model (SM). Assuming JUNO can measure Δm_{21}^2 and Θ_{12} by subpercent precision and assuming SM as the null hypothesis, we study the possibility to constrain NSI parameters by the future solar neutrino experiments such as DUNE, HK and MICA and present excluded region in NSI parameter space, ϵ_N and ϵ_D. For this purpose, we study the effect of NSI on solar neutrino propagation in the Sun and Earth and explore the dependence of the day-night asymmetry on the NSI parameters. we also study the effect of NSI at the detector on the simulated data for these experiments.

I. INTRODUCTION

Neutrino oscillation is well established by the data from a plethora of neutrino experiments using solar, atmospheric, reactor, and accelerator neutrino experiments over the last two decades [1]. The standard three flavor neutrino oscillation paradigm (standard paradigm) includes three active neutrinos that are linear combinations of three neutrino mass states. In the standard paradigm, there are three mixing angles θ_{12}, θ_{13}, θ_{23}, two mass-squared differences Δm_{31}^2, Δm_{21}^2 and one Dirac type CP phase δ_{CP}. Most of the oscillation parameters have been measured with fairly good precision [2–4]; However, there are some unknown quantities, namely, the value of the Dirac CP phase δ_{CP}, sign of $\Delta m_{31}^2 > 0$ and the octant of θ_{23}. To determine the unknown neutrino oscillation parameters, experiments with high statistics, such as JUNO [5], T2HK [6], and DUNE [7], have been proposed.

One way to test the standard paradigm is to measure the neutrino oscillation probabilities and compare the observed pattern with the expectations from standard paradigm. If the expectations from standard paradigm do not match the observed patterns, one can deduce that there is some unknown new physics beyond standard paradigm.

The framework of nonstandard neutrino interaction (NSI) provides one model-independent way to extend the standard model to quantify new physics in the neutrino sector as well as explaining neutrino mass. NSI was explored as a solution to the solar neutrino problem [8], and their impact on the oscillations of solar neutrinos [9], atmospheric neutrinos [10], and accelerator neutrinos [11] have been explored in the literature. Moreover, several consequences of NSI to DUNE were also explored in [12,13]. Moreover, there is a tension between the mass-squared difference obtained from the solar neutrino observations and the one from the KamLAND experiment. As studied in [14], one proposed solution is the sterile neutrino oscillation with the mass-squared difference of order of $O(10^{-5})$ eV^2, which is the so-called super light sterile neutrino scenario (SSNS). Another possibility is that the tension can be resolved by introducing the flavor-dependent NSI in neutrino propagation [15,16].

The Jiangmen Underground Neutrino Observatory (JUNO), the future reactor experiment with the baseline of 50 km is going to provide the possibility to measure Δm_{21}^2 and θ_{12} to the percent level [17] while not sensitive to the NSI parameters due to its short baseline and low neutrino energy [18]. The potential of JUNO to test SSNS is studied in [19].

In this work, we investigate how well precision measurements of oscillation probabilities at JUNO can be used to probe the existence of NSI. We consider future solar neutrino experiments, DUNE and HK in addition to the proposed solar neutrino experiment, MICA and explore the potential of these experiments in resolving standard

parameter degeneracies in the presence of NSI. Here we discuss the matter effect caused by NSI in the future solar neutrino experiments, using precision measurements of oscillation probabilities at JUNO.

Since solar neutrino oscillation probabilities are highly dependent on the NSI parameters due to the matter effect, with precise measurement of Δm_{21}^2 and θ_{12} by JUNO, we can investigate how well the future solar neutrino observatories can constrain nonstandard neutrino interaction parameters. Also, considering the day-night asymmetry of solar neutrino, we study the dependence of the day-night asymmetry on the NSI parameters. In addition, we explore the effect of NSI on the neutrino detection for HK and MICA detectors experiments which are water Cerenkov detectors [20].

For simplicity, we assume the same NSI couplings to electron, up quark, and down quark. As it is discussed in detail, assuming nonstandard couplings to electrons will affect the electron-neutrino scattering cross section and can lead to NSI at the HK and MICA detectors.

The paper is organized as follows. In Sec. II, we discuss the NSI Lagrangian and its effect on solar neutrino oscillation. In Sec. III, we discuss the details of different experiments and our simulation. In Sec. IV, we present our results. We briefly discuss our results in Sec. V.

II. NEUTRINO OSCILLATION FRAMEWORK WITH NSI

Neutral current (NC) NSI can be written as an effective four fermion operator

$$\mathcal{L}_{\text{NSI}} = -2\sqrt{2}G_F \epsilon_{\alpha\beta}^{fP}(\bar{\nu}_\alpha \gamma^\mu \nu_\beta)(\bar{f}\gamma_\mu P f), \qquad (1)$$

where f is a charged fermion, $P = (L, R)$ and $\epsilon_{\alpha\beta}^{fP}$ are dimensionless parameters encoding the deviation from standard interactions and G_F is the Fermi coupling constant. Constraints on $\epsilon_{\alpha\beta}$ have been discussed in many references. For instance, there are bounds from atmospheric neutrinos [21–24], from e^+e^- colliders [25], from the compilation of various neutrino data [26,27], from solar neutrinos [28–30], from $\nu_e e$ or $\bar{\nu}_e e$ scatterings [30], from solar, reactor, and accelerator neutrinos [31,32]. In addition, NSI has been studied in the context of long-baseline experiments [12,33,34].

NSI can be induced by the new physics beyond the standard model, by integrating out the heavier mediator fields which can generate the dimension-6 [35] and dimension-8 [36] effective operators. For a detailed review see Refs. [37,38].

The neutral current NSI (NC NSI) affect the neutrino oscillation in matter via forward elastic scattering. NC NSI also can affect the neutrino detection via neutrino electron scattering. In this work, we consider the effect of NSI on solar neutrinos for three cases: (i) through their propagation in the Sun, (ii) through their propagation in the earth, and (iii) by water Cherenkov detectors.

A. Propagation of neutrinos in the Sun in the presence of NSI

In the flavor basis, the flavor change of neutrinos through the propagation can be written as

$$i\frac{d}{dx}\psi_\nu = H\psi_\nu \qquad (2)$$

where the total Hamiltonian includes the vacuum effect, standard matter effect or MSW effect and NSI matter effect

$$H = H_{\text{vac}} + H_{\text{mat}}^{\text{MSW}} + H_{\text{mat}}^{\text{NSI}} \qquad (3)$$

The vacuum term includes six parameters, Δm_{21}^2, Δm_{31}^2, θ_{12}, θ_{13}, θ_{23}, δ_{CP} and is given by

$$H_{\text{vac}} = U\text{diag}\left(0, \frac{\Delta m_{21}^2}{2E_\nu}, \frac{\Delta m_{31}^2}{2E_\nu}\right)U^\dagger \qquad (4)$$

where U is the standard Pontecorvo-Maki-Nakagawa-Sakata mixing matrix, $U = R_{23}\Gamma_\delta R_{13}\Gamma_\delta^\dagger R_{12}$, where R_{ij} represents a real rotation by an angle θ_{ij} in the ij plane, $\Gamma_\delta = \text{diag}(1, 1, e^{i\delta})$. The Hamiltonian of standard matter effect is given by $H_{\text{mat}}^{\text{MSW}} = \sqrt{2}G_F N_e \text{diag}(1, 0, 0)$, where N_e is the number density of electron in the medium. Moreover, the NSI matter effect is given by

$$H_{\text{mat}}^{\text{NSI}} = \sqrt{2}G_F \sum_{f=e,u,d} N_f \begin{pmatrix} \epsilon_{ee}^f & \epsilon_{e\mu}^f & \epsilon_{e\tau}^f \\ \epsilon_{e\mu}^{f*} & \epsilon_{\mu\mu}^f & \epsilon_{\mu\tau}^f \\ \epsilon_{e\tau}^{f*} & \epsilon_{\mu\tau}^{f*} & \epsilon_{\tau\tau}^f \end{pmatrix}. \qquad (5)$$

It is possible to define NSI parameter in the medium

$$\epsilon_{\alpha\beta} \equiv \sum_{f=e,u,d} \left\langle \frac{N_f}{N_e} \right\rangle \epsilon_{\alpha\beta}^f = \epsilon_{\alpha\beta}^e + Y_u \epsilon_{\alpha\beta}^u + Y_d \epsilon_{\alpha\beta}^d \qquad (6)$$

where Y_α is the ratio of averaged fermion number density over electron number density in the medium. In the sun $Y_u \approx 2$ and $Y_d \approx 1$ and in the earth $Y_u \approx Y_d \approx 3$.

In order to study the effect of the NSI on the solar neutrinos, we can reduce the 3×3 Hamiltonian in Eq. (3), to an effective 2×2 Hamiltonian to obtain the survival probability. To study the propagation of solar neutrinos it is possible to work in the one mass dominance approximation that is given by [39] $\frac{\Delta m_{31}^2}{E_\nu} \gg G_F N_e$. In this approximation, the effective 2×2 Hamiltonian is given by [40]

$$H_{\text{vac}}^{\text{eff}} = \frac{\Delta m_{21}^2}{4E_\nu} \begin{pmatrix} -\cos 2\theta_{12} & \sin 2\theta_{12} \\ \sin 2\theta_{12} & \cos 2\theta_{12} \end{pmatrix}, \qquad (7)$$

$$H_{\text{mat}}^{\text{eff}} = \sqrt{2} G_F N_e(r) \begin{pmatrix} c_{13}^2 & 0 \\ 0 & 0 \end{pmatrix}$$

$$+ \sqrt{2} G_F \sum_f N_f(r) \begin{pmatrix} -\epsilon_D^f & \epsilon_N^f \\ \epsilon_N^{f*} & \epsilon_D^f \end{pmatrix}. \qquad (8)$$

The coefficients ϵ_D^f and ϵ_N^f are given concerning the original parameters $\epsilon_{\alpha\beta}^f$ as the following [15]

$$\epsilon_D^f = -\frac{c_{13}^2}{2}(\epsilon_{ee}^f - \epsilon_{\mu\mu}^f) + \frac{s_{23}^2 - s_{13}^2 c_{23}^2}{2}(\epsilon_{\tau\tau}^f - \epsilon_{\mu\mu}^f)$$
$$+ \text{Re}[c_{13}s_{13}e^{i\delta}(s_{23}\epsilon_{e\mu}^f + c_{23}\epsilon_{e\tau}^f) - (1 + s_{13}^2)c_{23}s_{23}\epsilon_{\mu\tau}^f], \qquad (9)$$

$$\epsilon_N^f = c_{13}(c_{23}\epsilon_{e\mu}^f - s_{23}\epsilon_{e\tau}^f)$$
$$+ s_{13}e^{-i\delta}[s_{23}^2\epsilon_{\mu\tau}^f - c_{23}^2\epsilon_{\mu\tau}^{f*} + c_{23}s_{23}(\epsilon_{\tau\tau}^f - \epsilon_{\mu\mu}^f)]. \qquad (10)$$

Then the effective Hamiltonian can be diagonalized as [41]

$$U' = \begin{pmatrix} \cos \tilde{\theta}_{12} & \sin \tilde{\theta}_{12} e^{-i\phi} \\ -\sin \tilde{\theta}_{12} e^{i\phi} & \cos \tilde{\theta}_{12} \end{pmatrix}, \qquad (11)$$

where

$$\tan 2\tilde{\theta}_{12} = \frac{|\sin 2\theta_{12} + 2\hat{A}_E \epsilon_N|}{\cos 2\theta_{12} - \hat{A}_E(c_{13}^2 - 2\epsilon_D)}, \qquad (12)$$

and

$$\phi = -\text{Arg}(\sin 2\theta_{12} + 2\hat{A}_E \epsilon_N). \qquad (13)$$

Considering this effective Hamiltonian and one mass dominance approximation, survival probability reduces to [40]

$$P(E) = \frac{1}{2}c_{13}^4[1 + \cos 2\theta_{12} \cos 2\bar{\theta}_{12}^m(E)] + s_{13}^4, \qquad (14)$$

where $\cos 2\bar{\theta}_{12}^m$ is the mixing parameter averaged over the boron neutrino production region in the Sun and is given by [42]:

$$\cos 2\bar{\theta}_{12}^m \approx \frac{\cos 2\theta_{12} - c_{13}^2 \bar{\epsilon}_\odot}{\sqrt{(\cos 2\theta_{12} - c_{13}^2 \bar{\epsilon}_\odot)^2 + \sin^2 2\theta_{12}}}. \qquad (15)$$

Here

$$\bar{\epsilon}_\odot \equiv \frac{2\bar{V}_\odot E}{\Delta m_{21}^2} \qquad (16)$$

and $\bar{V}_\odot$ is the averaged matter potential in the ^{8}B neutrino production region.

B. Day-night asymmetry

In principle, matter effects on neutrino oscillation can induce a difference between day and night rates. This occurs because neutrinos which are detected during the day, travel only through the Sun, while neutrinos detected during the night pass through the Earth's matter in addition to propagating through the Sun. This difference is quantified by the so-called day-night asymmetry. The difference of survival probability during night and day is given by [41,43]

$$\Delta P(E,\eta) = P_N - P_D$$
$$= \kappa(E)\left[\int_0^L dx V(x) \sin \phi^m(L - x, E) + I_2\right]. \qquad (17)$$

Here

$$\kappa(E) \equiv -\frac{1}{2}c_{13}^4 \cos 2\tilde{\theta}_{12}^s \sin 2\theta_{12}(\sin 2\theta_{12}(c_{13}^2 - 2\epsilon_D^E)$$
$$+ 2\cos 2\theta_{12}\epsilon_N^E) \qquad (18)$$

and the second term I_2 is a correction of the order ϵ^2 and is given by

$$I_2 = \frac{1}{2}\cos 2\theta_{12}\left(\int_0^L dx V(x) \cos \phi^m(L - x)\right)^2, \qquad (19)$$

$\phi^m(L - x, E)$ is the adiabatic phase acquired from a given point of trajectory x to a detector at L and is given by [43]

$$\phi^m(L - x, E) \equiv \int_x^L dx \Delta_{21}^m(x) \qquad (20)$$

where

$$\Delta_{21}^m = \Delta_{21}\sqrt{(\cos 2\theta_{21} - (c_{13}^2 - 2\epsilon_D^E)a_{CC}^E)^2 + |\sin 2\theta_{12} + 2a_{CC}^E\epsilon_N^E|^2} \approx \Delta_{21}(1 - c_{13}^2 \cos 2\theta_{12} a_{CC}^E) \qquad (21)$$

and $a_{CC}^E \equiv 2V(x)E/\Delta m_{21}^2$ and $\Delta_{21} \equiv \Delta m_{21}^2/4E$. As discussed in [43] I_2 is very small and we can neglect it in our calculations. For a constant density

$$\Delta P(E,\eta) = -\frac{1}{2}c_{13}^6 \cos 2\bar{\theta}_{12}^\odot(E)\sin^2 2\theta_{12} \times \left(\frac{a_{CC}}{1 - c_{13}\cos(2\theta_{12})a_{CC}}(1 - \cos(L\Delta_{21}(1 - c_{13}\cos(2\theta_{12})a_{CC})) \right) \quad (22)$$

where η is the nadir angle and

$$L = \cos\eta. \quad (23)$$

Considering the effective resolution function $g(E_r,E)' = g(E_r,E)\sigma(E)f_B(E)$, where $\sigma(E)$ is the neutrino interaction cross section and $f_B(E)$ is the flux, and plugging expression for $\Delta P(E)$, we have the following integral

$$I_\Delta(E_r) \equiv \int dEg'_\nu(E_r,E)\Delta P(E)$$
$$= \int_0^L dxV(x)\int_0^{E_B} dEg'_\nu(E_r,E)\sin\phi^m(L - x, E) \quad (24)$$

where we permuted integration over x and E. Let us introduce the attenuation factor $F(L - x)$ substituting the integral over E in Eq. (24) by

$$F(L - x)\sin\phi^m(L - x, E_r)$$
$$= \int dEg'_\nu(E_r,E)\sin\phi^m(L - x, E). \quad (25)$$

In general, this equality cannot be satisfied, but it is valid for special cases and under integral over x. Then the integral (24) becomes

$$I_\Delta(E_r) = \int dxV(x)F(L - x)\sin\phi^m(L - x, E_r). \quad (26)$$

For the ideal resolution, $g(E_r,E) = \delta(E_r - E)$, the Eq. (25) gives $F(L - x) = 1$ which means that attenuation is absent.

For the Gaussian energy resolution function the attenuation factor is given by

$$F(d) \simeq e^{-2(\frac{d}{\lambda_{att}})^2} \quad (27)$$

where

$$\lambda_{att} \equiv l_\nu \frac{E}{\pi\sigma_E} \quad (28)$$

is the attenuation length, and l_ν is the oscillation length in vacuum

$$l_\nu = \frac{4\pi E}{\Delta m_{21}^2}. \quad (29)$$

As can be seen in Eq. (27), for d much larger than λ_{att} (remote deep interiors), $F(d)$ goes to zero, while for d and λ_{att} at same order (the shallower interior), $F(d)$ becomes large; Thus, day-night asymmetry depends on the shallower interior more than deeper interior of the Earth.

Day-night asymmetry is defined as

$$A_{ND}(E_r,\eta) \equiv \frac{N_N}{N_D} - 1 \quad (30)$$

where

$$N_{D(N)} = A\int dEg_\nu(E^r,E)\sigma(E)f_B(E)\Delta P(E)_{D(N)} \quad (31)$$

where A is the factor which includes characteristics of detection.

The averaged over the year asymmetry is given by integrating A_{DN} multiplied by the exposure (weight) function $W(\eta)$ over nadir angle.

$$\bar{A}_{DN} = \int d\eta W(\eta)A_{DN}(\eta). \quad (32)$$

C. NSI detection

The differential cross section of neutrino electron scattering as a function of electron kinetic energy is well known and is given by [20]

$$\frac{d\sigma}{dT}(E_\nu, T_e)$$
$$= \frac{2G_F^2 m_e}{\pi}\left[(g_1)^2 + (g_2)^2\left(1 - \frac{T_e}{E_\nu}\right)^2 - g_1 g_2\frac{m_e T_e}{E_\nu^2} \right], \quad (33)$$

where T_e is the electron recoil energy, m_e is the electron mass, and E_ν is the initial neutrino energy. and g_1, g_2 are related to the SM neutral current couplings of the electron and are given by

$$g_1^{\nu_e} = g_2^{\bar{\nu}_e} = \frac{1}{2} + \sin^2\theta_W = 0.73 \quad (34)$$

$$g_2^{\nu_e} = g_1^{\bar{\nu}_e} = g_2^{\nu_\mu} = g_1^{\bar{\nu}_\mu} = \sin^2\theta_W = 0.23 \quad (35)$$

$$g_1^{\nu_\mu} = g_2^{\bar{\nu}_\mu} = -\frac{1}{2} + \sin^2\theta_W = -0.27. \quad (36)$$

The total cross section of neutrino electron scattering as a function of energy threshold and neutrino energy is given by

$$\sigma(E_\nu, T_e^{\max}) = \frac{2G_F^2 m_e}{\pi} \left[(g_1^2 + g_2^2)(T_e^{\max} - T_e^{\text{th}}) \right.$$

$$\left. - \left(g_2^2 + g_1 g_2 \frac{m_e}{2E_\nu} \right) \right. \tag{37}$$

$$\left(\frac{T_e^{\max^2} - T_e^{\text{th}^2}}{E_\nu} \right) + \frac{1}{3} g_2^2 \left(\frac{T_e^{\max^3} - T_e^{\text{th}^3}}{E_\nu^2} \right) \right] \tag{38}$$

where

$$T_e^{\max}(E_\nu) = \frac{2E_\nu^2}{m_e + 2E_\nu}. \tag{39}$$

Considering the neutral current NSI with electron g_1^e and g_2^e modifies as following [20],

$$g_1^{e\,\text{NSI}} = g_1^e + \epsilon_{ee}^{eL} \tag{40}$$

$$g_2^{e\,\text{NSI}} = g_2^e + \epsilon_{ee}^{eR} \tag{41}$$

III. DETAILS OF EXPERIMENT AND OUR ANALYSIS

In this section we discuss the main results of our analysis and discuss the possibility to constrain NSI parameters, considering the future solar neutrino experiments, namely, DUNE, HK, and MICA. For the statistical inferences we have considered ten years of data taking for each detector. Hyper-Kamiokande (HK) will detect the solar neutrinos by neutrino-electron elastic scattering with 6.5 MeV threshold [44]. Considering 0.5 Mton fiduciary volume, we have calculated 200 events per day [45]. We have assumed the energy resolution of HK is $\sigma_E/E = 0.15$. DUNE will have fiducial volume 40 kt liquid argon. On the other hand, DUNE can detect solar neutrinos via charged current interaction

$$\nu_e + {}^{40}\text{Ar} \rightarrow {}^{40}\text{K} + e^-. \tag{42}$$
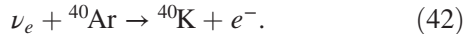
We consider the generic form of cross sections for interaction with nuclei

$$\sigma_{CC}(E) = A p_e E_e, \tag{43}$$

where A is a normalization factor (irrelevant for the relative excess), $E_e = E_\nu - \Delta M$, p_e is the electron momentum and $\Delta M = 5.8$ MeV is the reaction threshold [46]. Notice that only 9.7% of ^{8}B neutrinos have energy $E_\nu > 11$ MeV but due to strong energy dependence (43) the corresponding fraction of the detected events is 0.9. We find that about 27000 events of ν_e will be detected annually for $E_\nu > 11$ MeV in a 40 kt liquid argon detector considering

neutrino interaction with argon nuclei [43,46]. We have assumed the energy resolution of DUNE is $\sigma_E/E = 0.07$.

MICA is a proposed detector that will be located at Amundsen-Scott South Pole station [47], in the same place as ICECUBE. In our calculations we have taken the characteristics of MICA from Ref. [47], 10 Mton fiducial mass and 10 MeV energy threshold for the kinetic energy of the recoil electron. With these parameters, we find that about 5×10^5 solar νe- scattering events are expected per year. We have assumed the energy resolution of MICA will be $\sigma_E/E = 0.15$.

We have considered only solar boron neutrino flux from Ref. [42]. We have assumed solar neutrino parameters true value are $\Delta m_{21}^2 = 7.5 \times 10^{-5}$ and $\theta_{12} = 33.5°$. Our analysis shows that in the presence of NSI, Δm_{21}^2 and θ_{12} will be determined with a precision of 1.2×10^{-6} eV^2 and 0.07° respectively with JUNO after 10 years of data taking. We have considered all the details of JUNO the same as given in Refs. [18,19]. Since JUNO is going to determine these two parameters with very high precision, we can fix these parameters in our analysis. We have assumed the PREM model [48] for the Earth structure to calculate the day-night asymmetry. Besides, we have assumed the same details of analysis as given in Ref. [43]. For the statistical inferences we have considered Asimov data set approximation, and the true model is the standard model or $\epsilon_{\alpha\beta}^f = 0$. For statistical inferences for oscillation of the neutrinos in the sun, we have used the chi-squared method. We have neglected the matter effect in the earth or day-night asymmetry for constraining the parameters from the effect of NSI on the oscillation in the sun. We have assumed Gaussian distribution for statistical errors of day-night asymmetry. Moreover, in all of our calculation we have assumed $\epsilon_{\alpha\beta}^e = \epsilon_{\alpha\beta}^u = \epsilon_{\alpha\beta}^d$.

Comparing our results with the previous constraint on ϵ_D and ϵ_N which is presented in [49], our result shows that future solar neutrino experiment can constraint ϵ_D and ϵ_N 100 times more stringent than the previous results. More accurate measurement of θ_{12} and Δm_{21}^2 by JUNO and a large number of events collected by future solar neutrinos are responsible for this improvement. Moreover, our results show that the constraints on ϵ_{ee}^{eL} will be approximately five times more stringent than the current constraints on ϵ_{ee}^{eL} [20] at 3σ C.L. while the constraints on ϵ_{ee}^{eR} are in the same order.

IV. RESULTS

We have plotted $\cos 2\tilde{\theta}_{12}$ for different values of energy and ϵ in Fig. 1, considering $\epsilon_{\alpha\beta}^e = \epsilon_{\alpha\beta}^u = \epsilon_{\alpha\beta}^d$. As it is indicated in the plot, for values of $|\epsilon|$ less than 0.01, the ϵ_D is indistinguishable from ϵ_N in solar neutrino oscillation probability. For solar neutrinos with energies more than 10 MeV, there is a degeneracy between ϵ_D and ϵ_N for values of ϵ less than 0.03. In Fig. 2, we have plotted $\cos 2\tilde{\theta}_{12}$
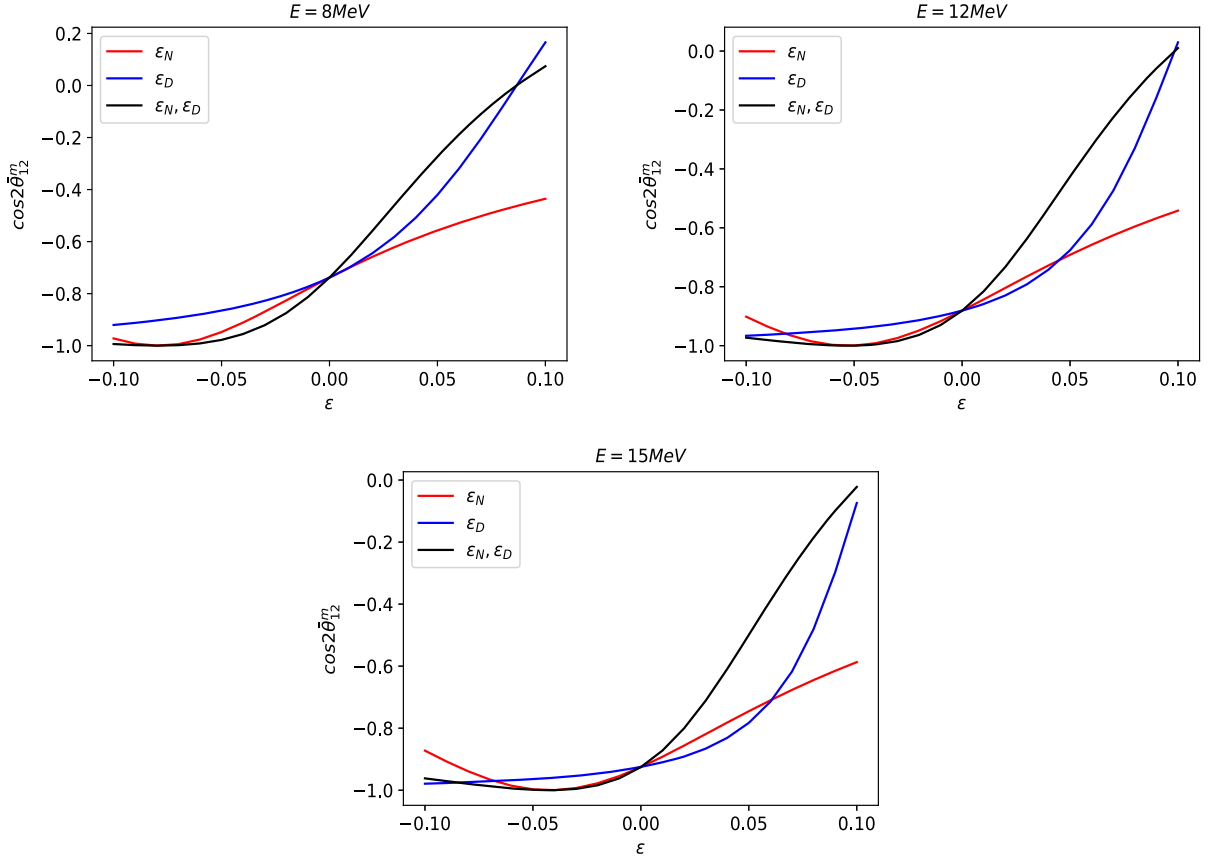
FIG. 1. $\cos 2\tilde{\theta}_{12}$ as a function of energy ϵ is plotted for three different neutrino energies of 8, 12, 15 MeV. We have assumed $\epsilon_e = \epsilon_u = \epsilon_d$. The blue, red, and black curves are plotted assuming $\epsilon_D \neq 0$, $\epsilon_N \neq 0$, and $\epsilon_D = \epsilon_N \neq 0$, respectively.

versus energy considering value of ϵ_D and/or ϵ_N is equal one.

Considering different solar neutrino observatories, DUNE, HK, MICA, and combination of DUNE and HK, the constraints on ϵ_D and ϵ_N after ten years of data taking are demonstrated in Fig. 3. As it is demonstrated the constraints on ϵ_D and ϵ_N will be of order of 0.01. As

FIG. 2. $\cos 2\tilde{\theta}_{12}$ versus energy is plotted assuming $\epsilon = 0.1$.

discussed before and it is demonstrated in Fig. 1, there will be a degeneracy between ϵ_D and ϵ_N, and also there is a strong anticorrelation between these two parameters.

We have calculated $\Delta P(E, \eta)$ numerically, considering the PREM model, for different values of energy. Since the peak of the events approximately corresponds to 12.5 MeV, we have demonstrated the results for this value of energy and for $L = 1000$ km and 4000 km in Fig. 4. As it is obvious the effect of ϵ_N is distinguishable from the effect of ϵ_D and the effect of ϵ_D is more significant on $\Delta P(\eta)$, while in comparison to ϵ_D, ϵ_N has a minor effect of day-night asymmetry. Considering other values of energy and baseline also leads to similar results.

We have also calculated $\bar{A}_{DN}$ for different values of ϵ_D and ϵ_N for three different experiments, DUNE, Hyper Kamiokande, and MICA, for $\theta_{12} = 33.5°$ and $\Delta m_{21}^2 = 7.5 \times 10^{-5}$ eV^2. The statistical precision measurement of DUNE, HK, and MICA will be 0.002, 0.001, and 0.0005 at 1σ C.L. after 10 years of data taking of solar neutrinos. The uncertainty of the value of A_{ND} from uncertainty of Δm_{21}^2 will be 0.0007, 0.0004, and 0.004 for DUNE, HK, and MICA respectively. Uncertainty of θ_{12} does not have any significant effect on A_{ND}. As it is indicated in Fig 5, the constraints on $|\epsilon_N|$, considering both

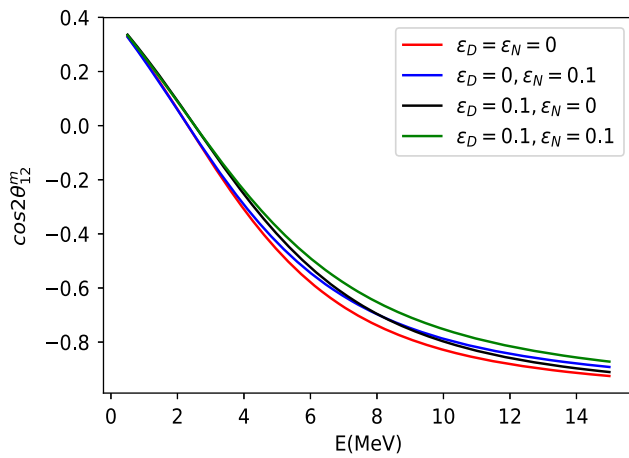FIG. 3. 1σ, 2σ, and 3σ allowed regions for ϵ_D as a function of ϵ_N at DUNE, HK, MICA, and combination of DUNE and HK assuming $\Delta m_{21}^2 = 7.5 \times 10^{-5}$ and $\theta_{12} = 33.5°$.

the statistical precision measurement and systematic uncertainty due to measurement of Δm_{21}^2, will be 0.014,0.014, and 0.007, and the constraints on $|\epsilon_D|$ are 0.004, 0.004, and 0.002, respectively with DUNE, HK and MICA.

Up to this point, in all our previous calculations for examining day-night asymmetry and oscillation of the neutrino in the sun, we have used the standard model cross section. In Fig. 6, total neutrino electron scattering cross section versus the neutrino energy is demonstrated considering different cases; The red curve is plotted

for HK experiment, considering standard model cross section for electron neutrinos, the blue curve indicates NC cross section for muon neutrinos, the green line is plotted considering NSI for electron neutrino interactions considering large value of $g_R^e = 0.5$ and the black line is plotted considering NSI for electron neutrino interactions considering large value of $g_L^e = 0.1$. We have considered the energy threshold of 6.5 MeV for the HK experiment. In the right panel, the results are indicated for MICA experiment, considering the energy threshold of
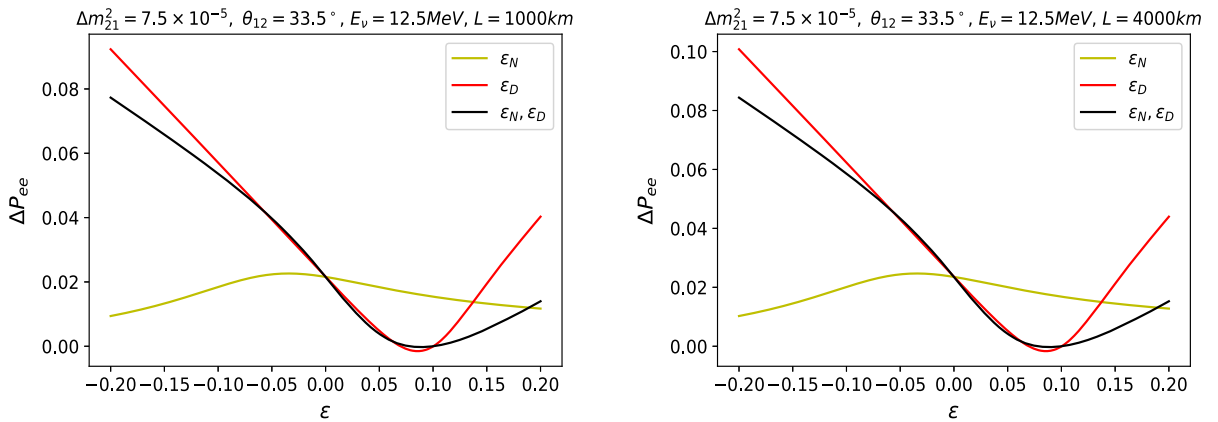

FIG. 4.   The differences in survival probability during night and day is plotted versus ϵ assuming neutrinos with the energy of 12.5 MeV. We have assumed $L = 1000$ km and $L = 4000$ km in the left and in the right panel, respectively. As can be seen, ϵ_D has a more significant effect on ΔP.
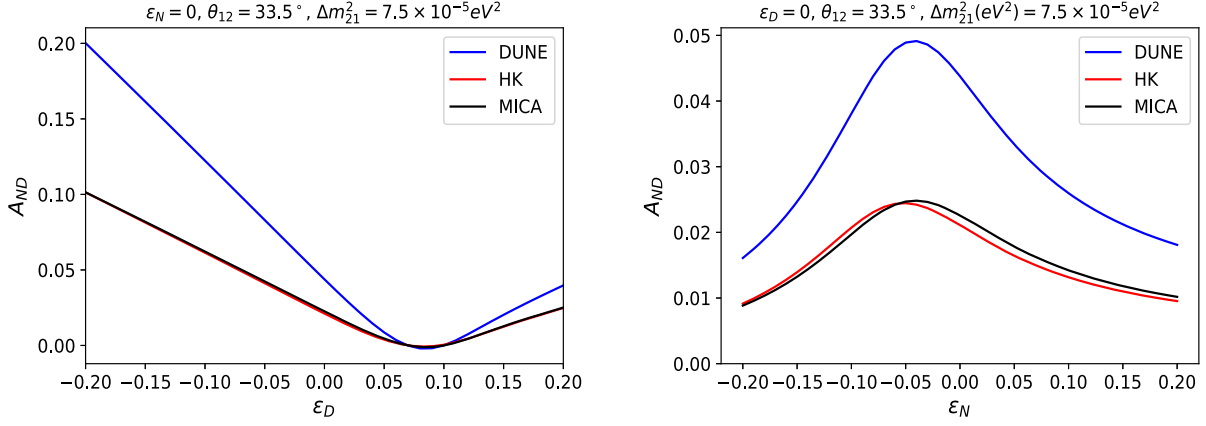
FIG. 5. A_{ND} as a function of ϵ is plotted for DUNE, HK, and MICA experiments.

10 MeV. As can be seen from the plot, the effect of g_R^e is minor.

If the future experiments establish a larger day-night asymmetry, similar to the value found by current Super-Kamiokande ($A_{ND} = 3.3 \pm 1 \pm 0.5$ percent) [50], considering that the prediction of best point fit of solar parameters from Kamland is 1.7 percent, such a significant difference cannot be explained by the allowed values of ϵ_N, but it can be explained by the allowed values of ϵ_D. Notice that both ϵ_N and ϵ_D will be constrained stringently by the oscillation of neutrinos in the Sun.

Moreover, it is interesting to investigate the effect of NSI at the detector in the simulated data for these experiments. We have demonstrated the potential of HK and MICA to constrain ϵ_{ee}^{eL} versus ϵ_{ee}^{eR} in Fig 7. As it can be seen from the plot, the constraint on ϵ_{ee}^{eL} is very stringent while in the case of ϵ_{ee}^{eR} is not.

The uncertainty of ϵ_{ee}^{eL} and ϵ_{ee}^{eR} can affect HK and MICA measurement of ϵ_D and ϵ_N from oscillation of the neutrino in the Sun. In the case of DUNE near detector, since the neutrino detection is via charged current interaction, adding the NC interaction does not affect the cross-section. However, if we consider charged current NSI, the NSI parameters will be constrained stringently by DUNE near detector down to the order 0.001 as studied in ref. [13]; Thus, considering CC NSI does not affect the cross section of DUNE and in consequence measurement of ϵ_{ee}^{eR} and ϵ_{ee}^{eL}.

In the case of MICA and HK, the uncertainties of the cross section and the flux do not affect day-night asymmetry. It can be seen from Eq. (30) where the uncertainties enter in both the denominator and in the numerator; Thus, the uncertainties of ϵ_{ee}^{eL} and ϵ_{ee}^{eR} do not affect the measurement of ϵ_N and ϵ_D in the day-night asymmetry. This is because cross section sensitivity to the energy is
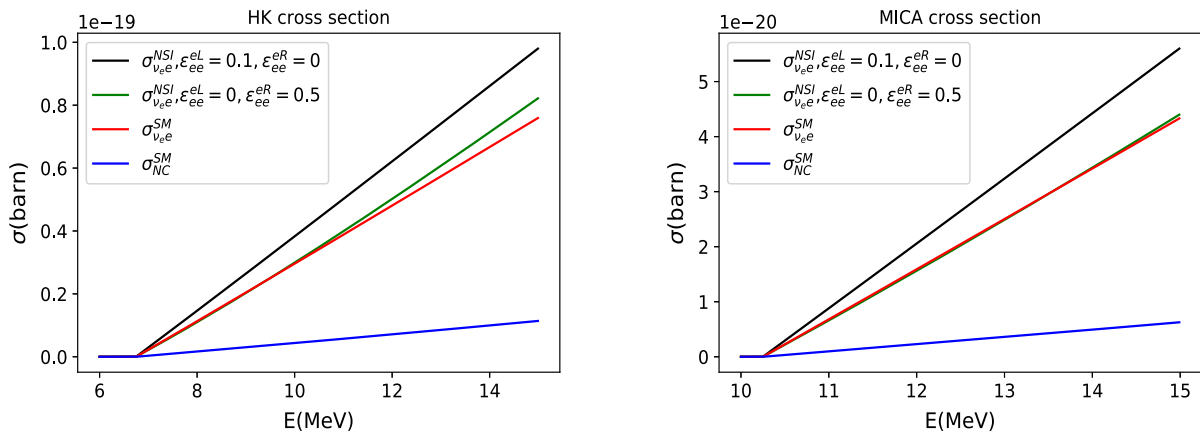

FIG. 6.   Total neutrino electron scattering cross section versus the neutrino energy. In the left panel, neutrino electron scattering cross section is plotted for HK experiment with the energy threshold of 6.5 MeV. the red line is plotted considering standard model cross section for electron neutrinos, the blue line indicates NC cross section for muon neutrinos, the green line is plotted considering NSI for electron neutrino interactions considering large value of $g_R^e = 0.5$ and the black line is plotted considering NSI for electron neutrino interactions considering large value of $g_L^e = 0.1$. In the right panel, neutrino electron scattering cross section is plotted considering MICA experiment with the energy threshold of 10 MeV. As can be seen from the plot, the effect of g_R^e is minor.
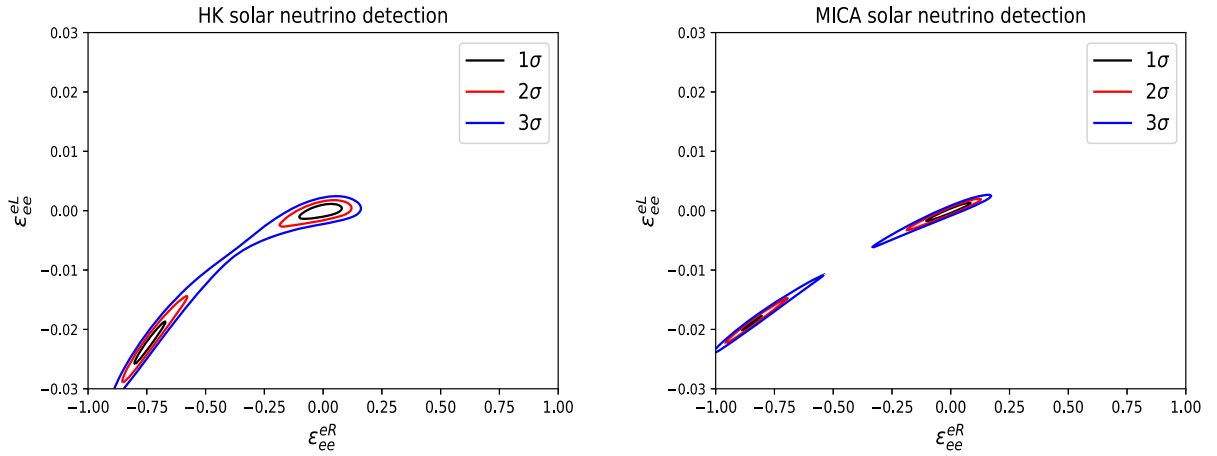
FIG. 7. 1σ, 2σ and 3σ allowed regions for ϵ_{ee}^{eL} as a function of ϵ_{ee}^{eR} for HK (left) and MICA (right).

negligible and the normalization factors cancel out in Eq. (30); Thus, the constraints from day-night asymmetry are not affected.

Since ϵ_{ee}^{eL} has a more significant impact of neutrino electron elastic scattering cross section than ϵ_{ee}^{eR}, to find the

impact of cross section uncertainty on ϵ_D and ϵ_N measurements from oscillation of the neutrinos in the Sun, we can explore the potential of HK and MICA using simultaneous measurement of ϵ_{ee}^{eL} and ϵ_D or by simultaneous measurement of ϵ_{ee}^{eL} and ϵ_N. The results are demonstrated in Fig. 8.

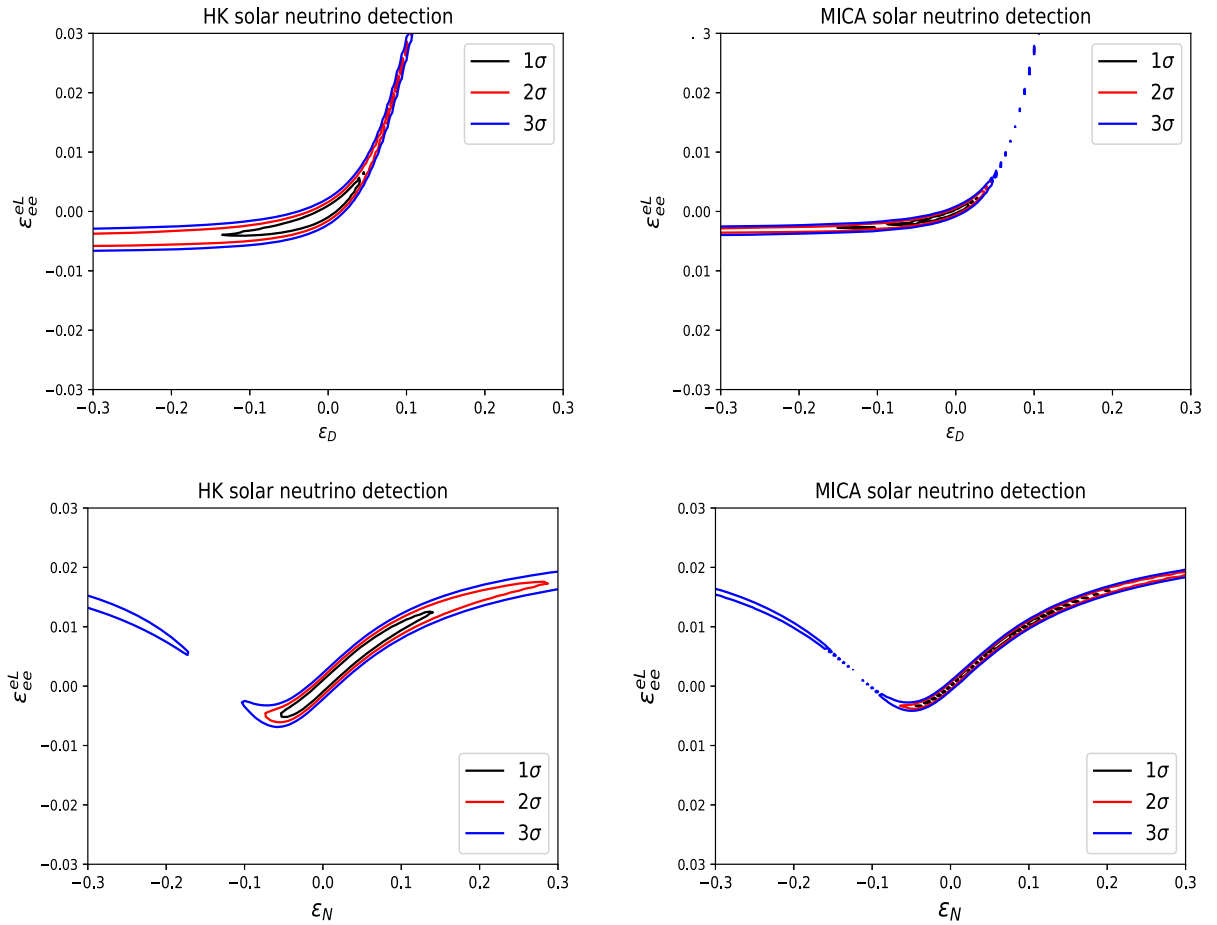FIG. 8. 1σ, 2σ and 3σ allowed region plotted for simultaneous measurement of ϵ_D and ϵ_{ee}^{eR} for HK (upper left panel) and for MICA (upper right panel). The lower panel indicates 1σ, 2σ and 3σ allowed region for the simultaneous measurement of ϵ_N and ϵ_{ee}^{eR} with HK (lower left) and MICA (lower right).

As it is shown, ϵ_{ee}^{eL} uncertainty has a huge impact on ϵ_D and ϵ_N measurement, with HK and MICA from neutrino oscillation in the Sun. However, as it is explained before, the constraints from day-night asymmetry are not affected. As it is indicated in Fig. 3, DUNE will constrain ϵ_D and ϵ_N down to 0.01 with 1σ, and ϵ_N and ϵ_D will be constrained by day-night asymmetry down to 0.01 and 0.004, respectively; Thus, ϵ_{ee}^{eL} will be constrained down to order of 0.001.

V. SUMMARY

We studied the sensitivities to NSI in the proposed next-generation solar neutrino observatories DUNE, HK, and MICA. The JUNO experiment will be able to measure Δm_{12}^2 and θ_{12} with less than one percent precision. On the other hand, having relatively low energy, the reactor experiment, JUNO is not sensitive to the standard and nonstandard matter effects. To study the effect of NSI parameters on the experimental performance, we considered this possible precise measurement of Δm_{12}^2 and θ_{12} by JUNO. We also assumed same NSI couplings for electron, up and down quarks ($\epsilon_{\alpha\beta}^e = \epsilon_{\alpha\beta}^u = \epsilon_{\alpha\beta}^d$).

Considering neutrino oscillation in the Sun, we demonstrated the constrains on ϵ_D and ϵ_N down to order of 0.01 at 3σ C.L. after ten years of data taking in Fig. 3 for future experiments DUNE, HK and the proposed MICA experiment in addition to the combination of DUNE and HK. We found that for the values of $|\epsilon|$ less than order of 0.01, the ϵ_D is indistinguishable from ϵ_N in solar neutrino oscillation probability as indicated in Fig. 1; We further studied the

day-night asymmetry parameters for three different experiments, DUNE, HK, and MICA. As we indicated in Fig 5, ϵ_D is significantly affected on day-night asymmetry while ϵ_N is not. We discussed that for the case of larger value of day-night asymmetry that may be established by future experiments, the allowed values of ϵ_N cannot explain such a huge difference while it can be explained by the allowed values of ϵ_D.

In addition, we studied the effect of NSI at the detector for the simulated data for these experiments. We demonstrated the potential of HK and MICA to constrain NSI. Our results show that while ϵ_{ee}^{eR} is weakly constrained, the constraint on ϵ_{ee}^{eL} is very stringent. We further studied the potential of HK and MICA simultaneous measurement of ϵ_{ee}^{eL} and ϵ_D and simultaneous measurement of ϵ_{ee}^{eL} and ϵ_N. We found that for HK and MICA experiments, ϵ_{ee}^{eL} uncertainty has a significant effect on ϵ_D and ϵ_N measurement considering neutrino oscillation in the Sun.

[1] C. Patrignani *et al.* (Particle Data Group), Chin. Phys. C **40**, 100001 (2016).

[2] F. Capozzi, E. Di Valentino, E. Lisi, A. Marrone, A. Melchiorri, and A. Palazzo, Phys. Rev. D **95**, 096014 (2017).

[3] P. F. de Salas, D. V. Forero, C. A. Ternes, M. Tortola, and J. W. F. Valle, Phys. Lett. B **782**, 633 (2018).

[4] I. Esteban, M. C. Gonzalez-Garcia, M. Maltoni, I. Martinez-Soler, and T. Schwetz, J. High Energy Phys. 01 (2017) 087.

[5] Z. Djurcic *et al.* (JUNO Collaboration), arXiv:1508.07166.

[6] S. Fukasawa, M. Ghosh, and O. Yasuda, Phys. Rev. D **95**, 055005 (2017).

[7] R. Acciarri *et al.* (DUNE Collaboration), arXiv:1512.06148.

[8] M. M. Guzzo, A. Masiero, and S. T. Petcov, Phys. Lett. B **260**, 154 (1991).

[9] P. I. Krastev and S. T. Petcov, Phys. Lett. B **299**, 99 (1993).

[10] M. C. Gonzalez-Garcia, M. M. Guzzo, P. I. Krastev, H. Nunokawa, O. L. G. Peres, V. Pleitez, J. W. F. Valle, and R. Zukanovich Funchal, Phys. Rev. Lett. **82**, 3202 (1999).

[11] A. Friedland and C. Lunardini, Phys. Rev. D **74**, 033012 (2006).

[12] M. Masud, A. Chatterjee, and P. Mehta, J. Phys. G **43**, 095005 (2016).

[13] P. Bakhti, A. N. Khan, and W. Wang, J. Phys. G **44**, 125001 (2017).

[14] I. Esteban, M. C. Gonzalez-Garcia, A. Hernandez-Cabezudo, M. Maltoni, and T. Schwetz, J. High Energy Phys. 01 (2019) 106.

[15] M. C. Gonzalez-Garcia and M. Maltoni, J. High Energy Phys. 09 (2013) 152.

[16] L. Wolfenstein, Phys. Rev. D **17**, 2369 (1978).

[17] Z. Djurcic *et al.* (JUNO Collaboration), arXiv:1508.07166.

[18] P. Bakhti and Y. Farzan, J. High Energy Phys. 07 (2014) 064.

[19] P. Bakhti and Y. Farzan, J. High Energy Phys. 10 (2013) 200.

[20] A. Bolanos, O. G. Miranda, A. Palazzo, M. A. Tortola, and J. W. F. Valle, Phys. Rev. D **79**, 113012 (2009).

[21] M. C. Gonzalez-Garcia, M. M. Guzzo, P. I. Krastev, H. Nunokawa, O. L. G. Peres, V. Pleitez, J. W. F. Valle, and R. Zukanovich Funchal, Phys. Rev. Lett. **82**, 3202 (1999).

[22] P. Lipari and M. Lusignoli, Phys. Rev. D **60**, 013003 (1999).

[23] N. Fornengo, M. C. Gonzalez-Garcia, and J. W. F. Valle, J. High Energy Phys. 07 (2000) 006.

[24] N. Fornengo, M. Maltoni, R. T. Bayo, and J. W. F. Valle, Phys. Rev. D **65**, 013010 (2001).

[25] Z. Berezhiani and A. Rossi, Phys. Lett. B **535**, 207 (2002).

[26] S. Davidson, C. Pena-Garay, N. Rius, and A. Santamaria, J. High Energy Phys. 03 (2003) 011.

[27] C. Biggio, M. Blennow, and E. Fernandez-Martinez, J. High Energy Phys. 08 (2009) 090.

[28] A. Friedland, C. Lunardini, and C. Pena-Garay, Phys. Lett. B **594**, 347 (2004).

[29] A. Palazzo and J. W. F. Valle, Phys. Rev. D **80**, 091301 (2009).

[30] J. Barranco, O. G. Miranda, C. A. Moura, and J. W. F. Valle, Phys. Rev. D **73**, 113001 (2006).

[31] J. Barranco, O. G. Miranda, C. A. Moura, and J. W. F. Valle, Phys. Rev. D **77**, 093014 (2008).

[32] F. J. Escrihuela, O. G. Miranda, M. A. Tortola, and J. W. F. Valle, Phys. Rev. D **80**, 105009 (2009); **80**, 129908(E) (2009).

[33] A. de Gouvea and K. J. Kelly, Nucl. Phys. **B908**, 318 (2016).

[34] R. Adhikari, S. Chakraborty, A. Dasgupta, and S. Roy, Phys. Rev. D **86**, 073010 (2012).

[35] W. Buchmüller and D. Wyler, Nucl. Phys. **B268**, 621 (1986).

[36] Z. Berezhiani and A. Rossi, Phys. Lett. B **535**, 207 (2002).

[37] T. Ohlsson, Rep. Prog. Phys. **76**, 044201 (2013).

[38] O. G. Miranda and H. Nunokawa, New J. Phys. **17**, 095002 (2015).

[39] M. Guzzo, H. Nunokawa, P. de Holanda, and O. Peres, Phys. Rev. D **64**, 097301 (2001).

[40] M. C. Gonzalez-Garcia and M. Maltoni, J. High Energy Phys. 09 (2013) 152.

[41] J. Liao, D. Marfatia, and K. Whisnant, Phys. Rev. D **92**, 073004 (2015).

[42] J. N. Bahcall, E. Lisi, D. E. Alburger, L. De Braeckeleer, S. J. Freedman, and J. Napolitano, Phys. Rev. C **54**, 411 (1996).

[43] P. Bakhti and A. Y. Smirnov, Phys. Rev. D **101**, 123031 (2020).

[44] Hyper-Kamiokande Collaboration, Reports No. KEK-PRE-PRINT-2016-21, No. ICRR-REPORT-701-2016-1.

[45] J. Liao, D. Marfatia, and K. Whisnant, Phys. Lett. B **771**, 247 (2017).

[46] A. Ioannisian, A. Smirnov, and D. Wyler, Phys. Rev. D **96**, 036005 (2017).

[47] S. Boser, M. Kowalski, L. Schulte, N. L. Strotjohann, and M. Voge, Astropart. Phys. **62**, 54 (2015).

[48] A. M. Dziewonski and D. L. Anderson, Phys. Earth Planet. Inter. **25**, 297 (1981).

[49] I. Esteban, M. C. Gonzalez-Garcia, M. Maltoni, I. Martinez-Soler, and J. Salvado, J. High Energy Phys. 08 (2018) 180.

[50] K. Abe et al. (Super-Kamiokande Collaboration), Phys. Rev. D **94**, 052010 (2016).